Quantification of Pain Severity using EEG-Based Functional Connectivity

P. Modares-Haghighi^{a}, R. Boostani^{a,*}, M. Nami^{b,c}, S. Sanei^{d}

[a] Department of Computer Science and Engineering, Shiraz University, Shiraz, Iran
[b] Department of Neuroscience, School of Advanced Medical Sciences and Technologies, Shiraz University of Medical Sciences, Shiraz, Iran
[c] Society for Brain Mapping and Therapeutics (SBMT), Los Angeles, CA, USA
[d] School of Science and Technology, Nottingham Trent University, Nottingham NG11 8NS, UK

Abstract

Background and Objectives: The traditional pain measures are qualitative and inaccurate. Therefore, electroencephalography (EEG) signals have been recently used and analyzed to differentiate pain from no-pain state. The challenge is emerged when the accuracy of these classifiers is not enough for differentiating between different pain levels. In this paper, we demonstrate that EEG-based functional connectivity graph is remarkably changed by increasing the pain intensity and therefore, by deriving informative features from this graph at each pain level, we finely differentiate between five levels of pain.

Methods: In this research, 23 subjects (mean age: 22 years, Std: 1.4) are voluntarily enrolled and their EEG signals are recorded via 29 electrodes, while they execute the cold pressure test. The signals are recorded two times from each case, while subjects press a button to annotate the EEGs into five pain levels. After denoising the EEGs, the brain connectivity graph in the Alpha band are estimated using partial directed coherence method in successive time frames. By observing the differences of connectivity graph features in different levels of pain, a bio-inspired decision tree (multilayer support vector machines) is proposed. Discriminant features are selected using sequential forward feature selection manner and the selected features are applied to the proposed decision tree.

Results: Classification result for differentiating between the pain and no-pain states provides 92% accuracy (94% sensitivity and 91% specificity), while for the five classes of pain, the proposed scheme generates 86% accuracy (90% sensitivity and 82% specificity), which is slightly decreased compared to the two-class condition. Moreover, the results are evaluated in terms of robustness against noise in different signal to noise ratio levels. Comparison results with previous research imply the significant superiority of the proposed scheme.

Conclusion: In this paper, we show that the elicited features from the filtered brain graph are able to significantly discriminate five different levels of pain. This is therefore the amount of co-activation between the brain regions (graph links) are significantly varied, as the pain feeling increases. Our observations are consistent with the physiological observations acquired from the images of functional magnetic resonance and magnetoencephalography.

Keywords : Brain connectivity graph, partial directed coherence, graph filtering, pain measurement

1. Introduction

Pain is an unpleasant emotional and sensual experience which leads to human protection against external injury. The primary stage in the pain perception mechanism is the activation of pain receptors in response to painful stimulus applied to peripheral nerves. The second stage is the transfer of pain, in which the pain message is transferred to higher brain centers such as thalamus, reticular formation, periaqueductal gray matter and hypothalamus and finally this message is transferred to the brain cortex. In this part, the regions of prefrontal cortex, anterior cingulate cortex, and somatosensory cortex insula are affected by pain [1]. In the last two decades, several attempts have been made for quantitative pain assessment, especially for patients who cannot speak or exhibit their pain intensity.

For instance, the intubated patients admitted to the intensive care unit (ICU), anesthetized patients in coma are unable to express their pain intensity. Although precise and quantitative pain assessment allows specialists to refine the treatment process, the current clinical pain measurement methods are mostly qualitative and therefore, their results suffer from a degree of subjectivity. The National Initiative on Pain Control (NIPC) suggests several diagnostic tools for specialists in order to measure the pain level. Amongst them, Wong-Baker FACES pain rating scale [2], visual analog scale [3] and verbal numerical rating scale [3] are recognized as the most popular and useful pain measures, which are all qualitative and no physiological based recording (e.g., brain signal) is carried out for this measurement. On the other hand, qualitative pain assessment highly depends on the subjects' tolerance in a way that a certain amount of mechanical/thermal/electrical pain stimulation [4-10] is not identically felt in different subjects.

*Corresponding author. E-mail address: boostani@shirazu.ac.ir

Among different noxious stimuli, the pain aroused by mechanical stimulation appears to be the highest. However, the side-effect of this stimulus is pretty high and volunteers do not like to experience it, whereas thermal stimulus has the lowest side-effect. By a deeper look through the literature, more than 90% of pain research projects use thermal stimulations like cold pressure test (CPT). In this test, a subject puts his/her hand into cold water (1.7 C) and holds his/her hand till the pain reaches up to the intolerable level, when the subject cannot continue the test and involuntarily takes his/her hand off the cold water. Feeling very cold water excites the pain-receptors as well as activating both central and sympatric nervous systems [11].

Investigations of the pain effect inside the brain have shown that a pain stimulus affects the cortical activity and desynchronizes the normal rhythms of electroencephalogram (EEG) signals. This desynchronization attenuates the EEG amplitude, specifically in the Alpha band while it alleviates the amplitude of Gamma band [12]. In spite of several attempts made to distinguish different levels of pain by analyzing EEG signals, the achieved results have provided acceptable performance just to differentiate pain and no-pain states [4,6,13]. In other words, by increasing the number of pain levels, the differentiation accuracy is significantly decreased.

Among several EEG features suggested for this purpose, the energy of EEG signals in the Delta and Alpha bands are the most conventional features [14]. In a few attempts, the coherence values in Delta, Alpha, and Beta bands between the left and right brain lobes are estimated to classify pain from no-pain states [15-21]. From another perspective, Zherdin and Schulz [13] applied the multivariate pattern analysis to EEG signals and then fed these features into a support vector machines (SVM) classifier. Their results on 22 subjects over the two states of pain and no-pain provided 83% classification accuracy, which leaves room for improvement.

In another research, Panavaranan and Wongsawat [4] recorded EEG signals of nine subjects under the CPT protocol. After denoising the signals, they extracted the spectral features from the EEGs. They finally applied them to a fuzzy-based SVM classifier with a polynomial kernel. Their results yielded 96.97% classification accuracy between the pain and no-pain states. Although this is a very good classification rate compared to previously developed methods, it stands for two-class classification only. It should be mentioned that although spectral features reveal the signals' content in the frequency domain and provide acceptable results (just in two-class pain problem), they cannot reveal other information captured in the EEGs such as complexity, the amount of nonlinearity, the degree of distribution symmetry and higher order statistics. Therefore, there is a possibility to enhance the results if more relevant features are extracted in conjunction with the spectral features. In another attempt, Toliyat and Vatankhah [6] applied wavelet coherence transform to the EEG signals of 13 subjects (recorded under the CPT protocol) to elicit the informative features and then applied them to a nonlinear SVM classifier, equipped with the radial basis function (RBF) kernel. They achieved 95% accuracy between the pain and no-pain states, which is an acceptable outcome. However, the dyadic decomposition of wavelet frequency interval is not certainly matched to the conventional EEG frequency bands [20]. In other words, the input signals are decomposed into a few scales by

the wavelet filters and then the coherence values are determined between the two-by-two channels over different scales. Moreover, SVM is a binary classifier and provides acceptable results for two-class problems but research findings [21] illustrate that the multi-class extension of SVMs cannot provide sufficiently accurate multi-level pain classification results.

Nezam et al. [22] recorded the EEG signals of 24 subjects and scored five levels of pain under the CPT protocol. During the process, they also eliminated the electrooculogram (EOG) and electromyogram (EMG) components by applying independent component analysis (ICA). Then, by tracing the grand-average brain map (just in the Delta and Alpha bands) for different pain levels, a hierarchical decision tree was devised based on the spectral features. In addition, other descriptive features such as fractal dimension, approximate entropy (ApEn) and spectral entropy were extracted and different subsets of features customized for the decision nodes of their proposed decision tree. Nonetheless, they achieved 62% accuracy for five pain levels and 83% for three levels. As we see, the accuracy of multi-class pain problems (62%) is still not convincing and a new category of methods is needed to achieve a higher accuracy.

Brain is the most complex organ in the human body, including several regions performing different functions. When the subject feels pain, the generated spikes from the brain sensory area activate the brain network [23]. To reveal the coactivation map of different brain regions, in response to different levels of pain, graph based structural and functional brain connectivity tools are seemed to be suitable candidates. In other words, the felt pain by harmonized activity of the brain network, connecting different regions, is encoded into a neuro-matrix. Using functional magnetic resonance imaging (fMRI), a horizon about the harmonic activity of the pain neuro-matrix is proposed to explain how the coactivity and correlation between different regions of the brain is created [26]. In this regard, functional connectivity of variations is shown in different pain states [25].

Functional connections during the pain feeling indicate the strength of temporal correlation between the activated brain regions. By estimating functional connectivity features, we can figure out how different regions of the brain are interacting with each other. To decode the functional information of the brain graph through a certain mental task, the graph theory is repeatedly deployed [26] to quantitatively illustrate the relation between different parts of the brain. According to this theory, the brain is assumed as a graph including nodes (EEG channels), located on the scalp, and links which represent functional connectivity among the nodes [27]. Topologic characteristics of the brain network can be examined in small, medium and large scales. In the large scale analysis, the whole brain is considered, in the medium scale a few regions of the brain are of interest while in the small scale, only one region of the brain is examined. There are several metrics to describe topologic characteristics (functional connectivity) of a graph.

In the brain, the experience of pain is associated with neuronal oscillations and synchrony at different frequencies over different scalp locations. However, here an overarching objective is to quantify the significance of these oscillations for different pain levels, which has not been done before. As such, our research focus is on evaluation of the pain-induced brain

oscillatory dynamics by exploiting the features of both local and global brain connectivity graphs, as physiologically meaningful EEG features.

Here, we have collected a new dataset containing the EEG signals of 23 healthy subjects who perform CPT for two times. After denoising the signals, they are filtered through only the Alpha band and the features like degree, betweenness, clustering coefficient, local and global efficiency of the brain graphs in two different scales are extracted. Next, the selected discriminant features are fed to our customized decision tree, which is a multilayer support vector machines classifier. This tree is structured by observing the differences of the brain connectivity graph among five pain levels. The results are compared to state-of-the-art methods for demonstrating the significant superiority of the proposed methodology.

The rest of this paper is organized as follows. Section II describes the collected dataset and its characteristics. Section III describes the preprocessing steps as well as explaining the implementations of functional connectivity graph features and our proposed classifier. Section IV illustrates the empirical results and discusses the pros and cons of the proposed method compared to state-of-the-art schemes on our dataset. Section V concludes the paper and opens a new horizon to the future of this work.

2. Data Acquisition

In this research, 23 right-handed volunteers are enrolled including 14 males and 9 females whose age is in the range of 20-25 years old (Mean: 22 years old) with relatively similar education level. No sign of sleep or cognitive/behavioral disorder, psychological and neurological disease, head trauma, chronic pain and also substance addiction, affecting the brain activity was observed in the participants.

In fact, to ascertain the subjects' status such as having psychological or neurological diseases, all individuals were initially screened by a clinical-cognitive neuroscientist for their health history, past medical history, and any medications they use. They also underwent neurological examination and cognitive assessment by the same expert after which they were granted clearance to participate in the study.

Individuals have an appropriate sleep in terms of quality just before the day of EEG recording (receiving score less than 8 in PIRS questionnaire and more than 7 in VAS) and avoid drinking tea and coffee. The minimum duration of the trial is 15 seconds. If any individual cannot tolerate this period of time, he/she has a chance to rule out. Individuals after receiving sufficient information about the research, fill up the testimonial acknowledged that they have voluntarily participated in this research project and can leave the trial at any stage of the test. EEG signals are recorded by 29 silver electrodes including one channel as the reference located between the eyebrows (FPz) and 28 channels (Fp1, Fp2, F7, F8, F3, Fz, F4, FC1, FC2, FC5, FC6, T7, T8, C3, Cz, C4, Cp5, CP6, CP1, CP2, P7, P8, PZ, P3, P4, O1, O2 and OZ) located on the scalp according to 10-20 EEG electrode positioning system [28-29]. The impedance of all of the electrodes is kept under 5 KΩ during the recording. The sampling rate is 512 Hz and the recorded signals are filtered by a Butterworth band pass filter with the cut-off frequencies of 0.5 and 45Hz. The pain is induced by CPT with 1.7 Celsius

degree. Before the signal recording, individuals' hand is put in the cold water once tentatively in a way that they can enounces their pain stages while each volunteer seats on a comfortable chair. EEGs are recorded from the individuals at the rest state (approximately 3 minutes) subsequently the left hand of the participants is put in the cold water. To avoid the results from being biased in favor of the pain class with higher population (no-pain class), we randomly select a short interval of their no-pain stage, where its length is approximately relative to the recording of the EEGs in the other pain classes. During the time that the left hand of each subject is in cold water, the signals are marked by a button located in the right hand of the participant (synchronized with the EEG recording) according to the intensity of the pain being felt include low, mid and high. Subjects press a bottom whenever they feel the level of pain is changed. By the passage of time, subjects cannot keep their hand in the cold water any longer and involuntarily take their hand out of the cold water. The recorded EEGs after feeling the high pain is labeled as the intolerable pain class. Regarding the differences between the participants' tolerance in response to a certain level of pain, the interval of each pain state varies from one to another and their no-pain intervals are selected accordingly.

3. Proposed Method

The road map of the proposed procedure is illustrated in Fig. 1, in which the recorded EEGs are passed through several stages including: preprocessing, brain graph creation, graph filtering, extracting graph connectivity metrics and finally the proposed bio-inspired decision tree classifier. What follows are the description of the mentioned phases.
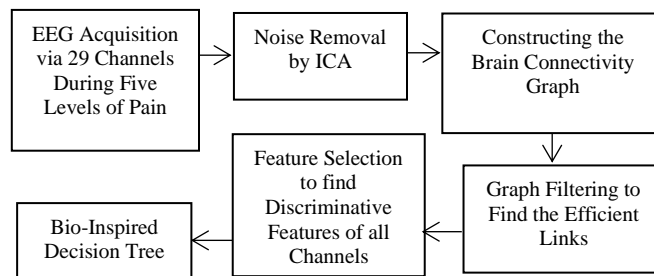

Fig. 1. Block diagram of the proposed framework

3.1. Preprocessing

The amplitude and frequency of EEGs vary in the range of 10–100 μV, and 0.5 to 60 Hz, respectively. Contraction of facial muscles followed by feeling of pain in conjunction with other movement artifacts lead to interfere of EMG and EOG signals as well as baseline variation into the content of EEGs.
For instance, baseline and EOG signals offend low frequency components of the EEGs, while EMG signals distort its high frequency content. Here, to remove these undesired components, spatial filtering is utilized, which contains three stages [28].

The recorded raw EEGs are decomposed into spatial components using second order blind identification (SOBI) algorithm. Then the fractal dimension of the decomposed

signals is determined. Fractal dimension of EOG sources is quite low because these sources contain low frequency and regular components while the background EEG contains more scattered frequency components that results in a higher fractal dimension value. To identify the EMG components, we have calculated the average power spectrum of the sources and compare them to the power spectrum of FP1 channel (nearest channel to the forehead muscle). Those sources which have the highest similarity with that of FP1 are removed as the EMG sources. Finally, the remained sources are projected back to the spatial domain. In addition, by filtering the reconstructed EEGs through a band-pass filter (0.5-45Hz) and a notch filter (50Hz), both baseline and power line are removed. The preprocessing phase is performed by the EEGLAB toolbox [27].

3.2. Creation of the brain graph

To construct the brain graph from the EEGs, assume that EEG channels of $X_1(t)$, $X_2(t)$, ..., $X_N(t)$ are considered as the N nodes. We set up a connection matrix $W_{N \times N}$, where each cell w_{ij} indicates the value of link between the nodes i and j.

The main graph-based methods to determine the functional connectivity in the time and frequency domains are granger causality (GC) and partial directed coherence (PDC), respectively [28-29]. PDC describes the relation between multivariate time series in the frequency domain which is based on the coherence analysis of the multivariate autoregressive models [30]. In comparison with the other functional connectivity schemes, it is demonstrated that PDC is more robust to noise and is not also affected by the volume conduction [34]. The PDC values are in the range of [0,1], where higher values indicate more interaction between two EEG channels. The multivariate autoregressive (MVAR) model with order p is described as follows:

$$X(t) = -\sum_{\tau=1}^{p} A(\tau)X(t-\tau) + E(t) \tag{1}$$

where $A(\tau) = \begin{bmatrix} a_{11}(\tau) & ... & a_{1N}(\tau) \\ ... & ... & ... \\ a_{N1}(\tau) & ... & a_{NN}(\tau) \end{bmatrix}$ are the matrix

coefficients of MVAR model at delay τ and E is the noise vector. The autoregressive coefficients of $a_{ij}(\tau)$, where $i,j=1, ..., N$, represents the affection of $x_j(t-\tau)$ on the $x_i(t)$. In other words, $a_{ij}(\tau)$ shows the amount of information flow of the jth signal to the ith signal. In this study, matrix A and the order of autoregressive model are estimated by the stepwise least square method [31] and Bayesian information criterion [32], respectively. The PDC of the channel j^{th} to the channel i^{th} in the frequency domain is defined as [28]:

$$PDC_{ij}(f) = \frac{A_{ij}(f)}{\sqrt{\sum_{k=1}^{N} A_{kj}(f)A_{kj}(f)}} \tag{2}$$

where $A(f)$ is the Fourier transform of the MVAR coefficients of $A(\tau)$. If the element $a_{ij}(f)$ in the matrix $A(f)$ is the Fourier transform of $a_{ij}(\tau)$ in the matrix $A(\tau)$. Therefore, we can have $a_{ij}(f) = \sum_{\tau=1}^{p} a_{ij}(\tau)e^{-l(2\pi/p)rf}$. Since the AR model is only valid for stationary signals, the EEG signals of all channels are segmented into successive windows (with 50% overlap), where the length of each window is selected one second to guarantee preserving the stationary property. After finding the directed functional connectivity of all channels through the time frames, we sketch the grand average (information flow graph) over the brain using the Econnectome software [37] for each pain level, separately in Fig. 2.
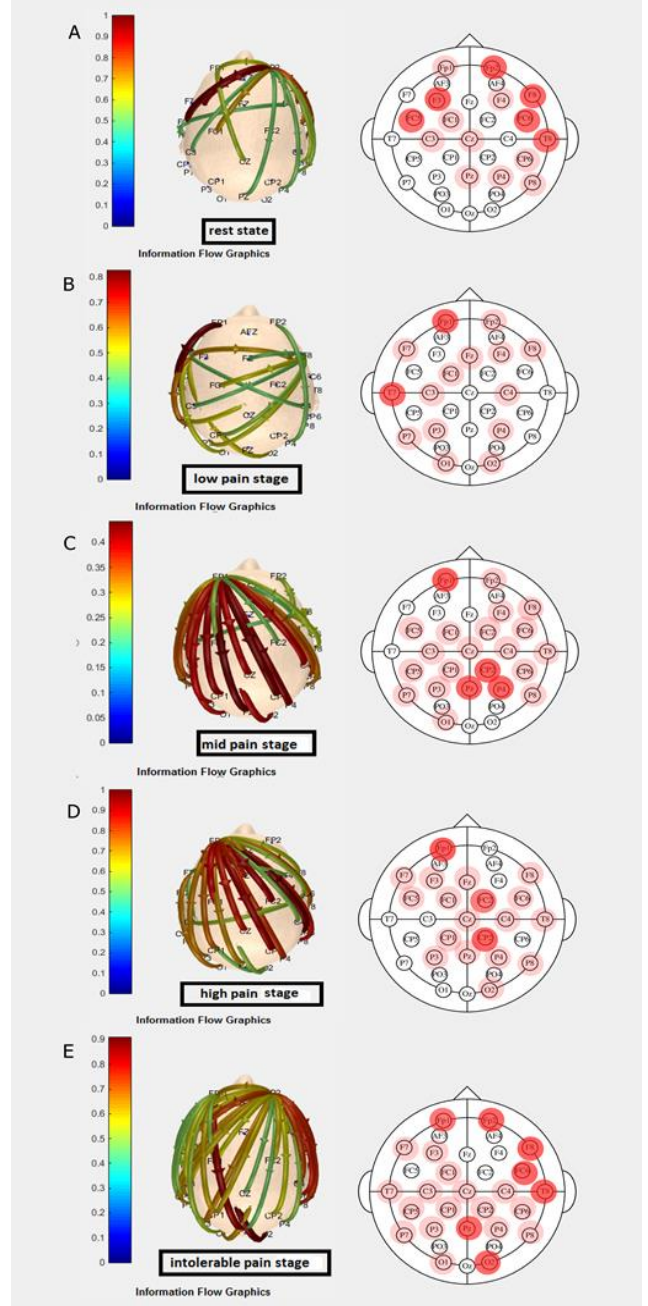

Fig. 2. Grand average brain graph in rest, low, moderate, high and intolerable pain states.

Fig. 2 demonstrates all the channels are involved in the recordings during rest, low, moderate, high and intolerable pain states. Nevertheless, in each state we have identified the

strongest connections between some channels as follows:

Rest stage: FP1, FP2, F8, F3, F4, T8, C3, P8, P4, FC1, CZ, PZ, FC5, FC6, CP6 with dominant connections amongst FP2, F8, F3, T8, FC5, FC6.

Low pain stage: FP1, FP2, F7, F8, F4, T7, C3, C4, P7, P3, P4, O1, O2, FC1, FZ, CP1 with dominant connections amongst FP1, T7.

Moderate pain stage: FP1, FP2, F8, F4, T8, C3, C4, P7, P8, P3, P4, O1, FC1, FC2, CZ, PZ, CP1, CP2, FC5, FC6, CP5, CP6 with dominant connections amongst FP1, PZ, CP2, P4.

High pain stage: FP1, F7, F8, F3, T8, C4, P8, P3, P4, O2, FC1, FC2, FZ, CZ, PZ, CP1,CP2, FC6, CP6 with dominant connections amongst FP1,FC2, CP2,CP6.

Intolerable pain stage: FP1, FP2, F7, F8, F3, T7, T8, C3, C4, P7, P8, P3, P4, O1, O2, FC1, CZ, PZ, CP1, CP2, FC5, FC6, CP5, CP6 with dominant connections amongst FP1, FP2, F8, T8, O2, PZ, FC6.

As illustrated in the Figure, the left frontopolar cortical region (FP1) appears to be the source for information flow in all stages of pain perception. The more intense the pain gets the flow of information and sensory motor rhythm coherence swing toward the right hemisphere.

3.3. Graph filtering

After determining connections between the graph nodes, some of the non-realistic links must be filtered because the values of elements in matrix $W_{N \times N}$ (functional connectivity graph) can be seriously affected by non-neurological disturbances such as additive noises [38]. In the cumulative thresholding method, the threshold value is chosen in a way that the connectivity matrix with densities of 10% to 90% of the strongest connections is determined [35].

To prone the graph, alternative windowed thresholding is used as an adaptive method, which determines the threshold within each time frame. For instance, the first graph is mapped from 10% of the strongest connections, the second graph from 10% of the strongest remnants and so on, such that the last graph is mapped from 10% of the weakest connections [36].

After filtering the connectivity graphs, we analyze them in the framework of large and small scales. In the large scale, the metrics (features) are extracted from the whole brain area, while in the small scale, the metrics are elicited from a single region of the brain (e.g., one node). To elicit meaningful features, the node degree, betweenness, clustering coefficients, local and global efficiency metrics are determined. These metrics are explained as follows.

3.4. Graph metrics

3.4.1. Degree

The node degree K_i is the number of links which are connected to the node i. Nonetheless, in directed graphs, the node degree has two parts:

The number of outgoing links $K_i^{out} = \sum_j a_{ij}$ and the number of incoming links to the node $K_i^{in} = \sum_j a_{ji}$, where a_{ij} is the connection status between i and j. When link (i, j) exists then

$a_{ij} = 1$; otherwise $a_{ij} = 0$. The total degree of node i is the summation of K_i^{out} and K_i^{in} [37]. The node degree is used for small scale graph analysis.

3.4.2. Betweenness

Betweenness is a metric, revealing the importance of a node in a graph, under the assumption that information primarily flows through the shortest paths between them. This feature is determined below:

$$b_i = \sum_{j,k \in N j \neq k} \frac{n_{jk}(i)}{n_{jk}} \tag{3}$$

where n_{jk} is the number of shortest paths that connecting j and k and $n_{jk}(i)$ is the number of shortest paths connecting j and k that passes through node i [37].

3.4.3. Efficiency

In the network field, the efficiency criterion measures how well the information is communicated between nodes. The concept of efficiency can be used locally or globally in a network. The global efficiency measures the performance of transferred information in the whole network, in which the information is simultaneously communicated. On the other hand, the local efficiency determines the resistance of a network against inefficiency in a small scale. The local efficiency of a node specifies the amount of transferred information by its neighbor, where the corresponding node is eliminated. The global efficiency of a network is defined as:

$$E = \frac{1}{N} \sum_{i \in N} E_i = \frac{1}{N} \sum_{i \in N} \frac{\sum_{j \in N \, j \neq i} d_{ij}^{-1}}{n - 1} \tag{4}$$

where E_i is the efficiency of node i, N is the set of all nodes in the network, n is the number of nodes contributing in determining E_i and d_{ij} is the shortest path between nodes i and j. The local efficiency is also defined as:

$$E_{loc} = \frac{1}{n} \sum_{i \in N} E_{loc,i} = \frac{1}{n} \sum_{i \in N} \frac{\sum_{j,h \in N \, j \neq i} a_{ij} a_{ih} [d_{jh}(N_i)]^{-1}}{k_i(k_i - 1)} \tag{5}$$

where $E_{loc,i}$ is the local efficiency of node i, and $d_{jh}(N_i)$ is the length of the shortest path between j and h, that contains only neighbors of i [38].

3.4.4. Clustering coefficient

This criterion gives a value for each node of a graph that determines its tendency to be a member of cluster. This coefficient is mathematically determined via the following relation [45]:

$$C_i = \frac{\sum_{j \neq i \, k \neq i,k \neq j} \sum (w_{ij}^{1/3} + w_{ji}^{1/3})(w_{ik}^{1/3} + w_{ki}^{1/3})(w_{jk}^{1/3} + w_{kj}^{1/3})}{2[(H^T + H)_i((H^T + H)_i - 1) - 2H_{ij}^2]} \tag{6}$$

where w_{ij} is the directed functional connectivity related to the nodes i and j. The nodes j and k are two neighbors of the node i

and H is the adjacency matrix ($H_{ij} = 1$ if $w_{ij} \neq 0$). The mean of clustering coefficient over the nodes is defined as:

$$C = \frac{1}{N}\sum_{i \in N} C_i \qquad (7)$$

3.5. Decision tree

Looking at Fig. 2, we can see a significant difference between the functional connectivity graph of the no-pain and the other pain states. Therefore, an SVM classifier is assigned to classify the no-pain from the other pain classes in the first decision node. Then, among the four remained classes, the intolerable pain graph has a significant difference with the graphs of the remained three classes. Similarly, a SVM is assigned for this task. In the next stage, the high pain is classified and finally the low and mid pain classes are classified according to the differences of the corresponding graphs. The proposed bio-inspired decision tree structure, which is a multilayer SVM, is shown in Fig. 3, where a SVM is assigned at each decision node.
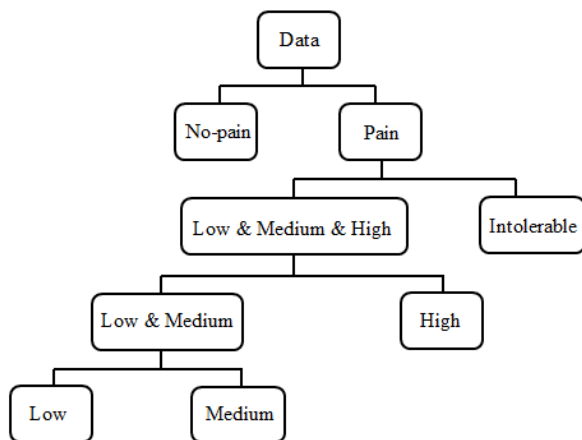

Fig. 3. Structure of the decision tree

4. Experimental Results

In this section the classification results of the proposed brain connectivity features for classifying the five classes of pain are presented. As we mentioned in the preprocessing section, the signals are all filtered only through the Alpha band (8-12Hz) because all of the pain detection studies emphasize the existence of distinguishable information within this band [46].

The EEG signals are de-noised using SOBI and afterward, the large and small scale graph connectivity features are extracted from the functional brain connectivity graphs in order to finely describe the state of pain. This is therefore pain is a sense followed by a motor reflex and any somatosensory process that can be screened by the interval between the Alpha and Beta bands called SMR (12 to 13 Hz). In fact, SMR is influenced by every sensory process, whether controlled (merely sensory) or not controlled (painful sense). Thus, we analyze just the Alpha band of EEG signals. Brain network graph requires two elements in order to be drawn. The number of effective EEG channels (nodes) is 28 [35-36] and links are

calculated through the Alpha band for successive one-second time frames with 50% overlap. Graphs' links are obtained through functional connectivity graph calculation which is a 28×28 matrix for each window along EEG [36]. Functional connectivity using PDC is determined [32]. In addition, we have used generative surrogate data method with 100 realizations for selecting the most important measured values with the confidence level of 99%. The values of directed connectivity of PDC are considered as features ($28 \times 28 = 784$ features) for distinguishing the two levels of pain and no-pain. This differentiation is performed via SVM classifier equipped with radial basis function (RBF) kernel. To achieve the best accuracy, the value of C is determined through the cross validation (5 folds). Due to facing with large number of features, we have used sequential floating forward selection (SFFS) as a search strategy to elicit a proper subset of features in a wrapper style, where the classifier feedback is used as the objective function. By eliciting the directed functional connectivity features, the no-pain class is classified from other pain classes and the results are presented in Table 1.

Table 1
The pain classification results by Using the PDC directed functional connectivity

Classified states	Accuracy ± std (%)	Specificity (%)	Sensitivity (%)
No-pain VS. Pain	92.75±0.0476	91.06	94.03

To filter the functional connectivity matrix with traditional cumulative thresholding method, the connection matrix elements with the density of 10%, 20%, …., 80% and 90% is respectively preserved [39]. Other elements are sequentially substituted with zero. In an alternative windowed thresholding method, the connection matrix is obtained in seven windows (levels of selection). Hence, we have: window#1 includes 1-10% of the strongest connections, window#2 indicates intermediate brain connections, window#3, 4, 5, 6 and 7 indicates weakest brain connections [40]. By having filtered functional connectivity matrix, we study the brain network in both large (metrics on the whole graph) and small (metrics on a single region) scales. Thereafter, we empirically calculate the degree, betweenness, clustering coefficient, local efficiency and global efficiency [41]. Except the global efficiency criterion, the other criteria include a vector with size: 1×28. In order to compare the extracted criteria from the functional connectivity matrix with the density of 90%, we have used the ANOVA test, and the results are presented in Fig. 4. The mean of the graph measures include clustering coefficient, local and global efficiency in five levels of pain over 23 subjects, with the densities of 10% to 90% are shown in Fig. 5, where the windowed connectivity matrix are extracted for 1-10% , 11-20% , 21-30%, 31-40%, 41-50%, 51-60%, 61-70%. Error bars demonstrate the standard deviation.

In this stage, the classification of no-pain class versus the other pain classes, the low-medium-high pain classes versus the intolerable pain classes, low-medium versus high pain classes and the low pain class versus the medium pain class are performed. SVM with RBF kernel is used for the classification

at each node. As we mentioned, SFFS is utilized to select the features [44].
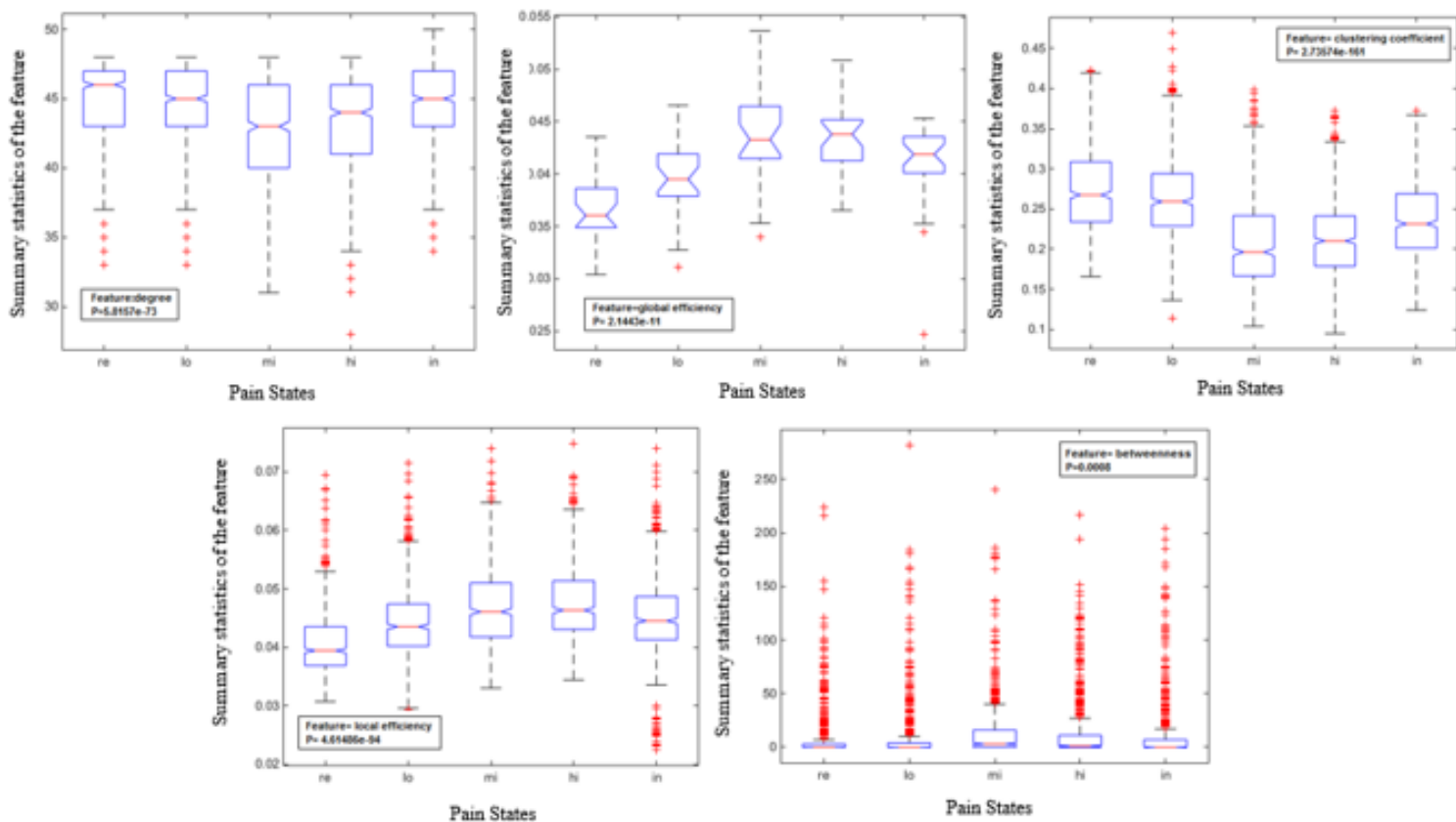

Fig. 4. Box plots of distribution of all different features in five pain states. The p-value and the examined features name is included in the text boxes of every different plot.

For classification, we divide our community into two groups: one validation group including 17 individuals and test group including 6 subjects. No over-fitting is occurred among the validation and test groups. K-fold method is used in the validation group, where K is considered as five. Therefore, the validation group is divided into five separate groups. Each time one of these five groups are put aside and the remaining groups are considered as the training group and a SVM classifier is trained and then the accuracy of test group is evaluated. This process is repeated five times. Parameter C has been chosen in the interval of 0.1 to 10 with steps of 0.05 in a way that the validation group achieves the most accuracy. For each functional connection matrix, 16 filtered matrices with traditional cumulative thresholding and alternative windowed thresholding methods are obtained. Now we have 16 functional communication matrices for each time frame which are filtered. All these stages are repeated for each functional communication matrix to discover which one is filtered. Here, we assess the classification accuracy over the one by one extracted features from the filtered connectivity matrix. The maximum accuracy belongs to the extracted criteria from the connectivity matrix

with the density of 90%. The maximum accuracy of the pain levels is related to following features which are listed in Table 2. The classification accuracy of the pain levels are demonstrated in Table 3.

Since the pain is continuously increased, we can divide this interval into three intervals in a way that we concatenate the low and moderate pain as one label and the high and intolerable pain states as the third label. Hence, we have three new labels including rest, moderate pain and high pain. The results for three-level and five-level pain classes are illustrated in Table 4. In order to compare the proposed method with state-of-the-art methods in this field, their results in terms of number of pain classes, the utilized EEG features and the classification accuracy are demonstrated in Table 4. It should be considered that the best result for each method is shown.
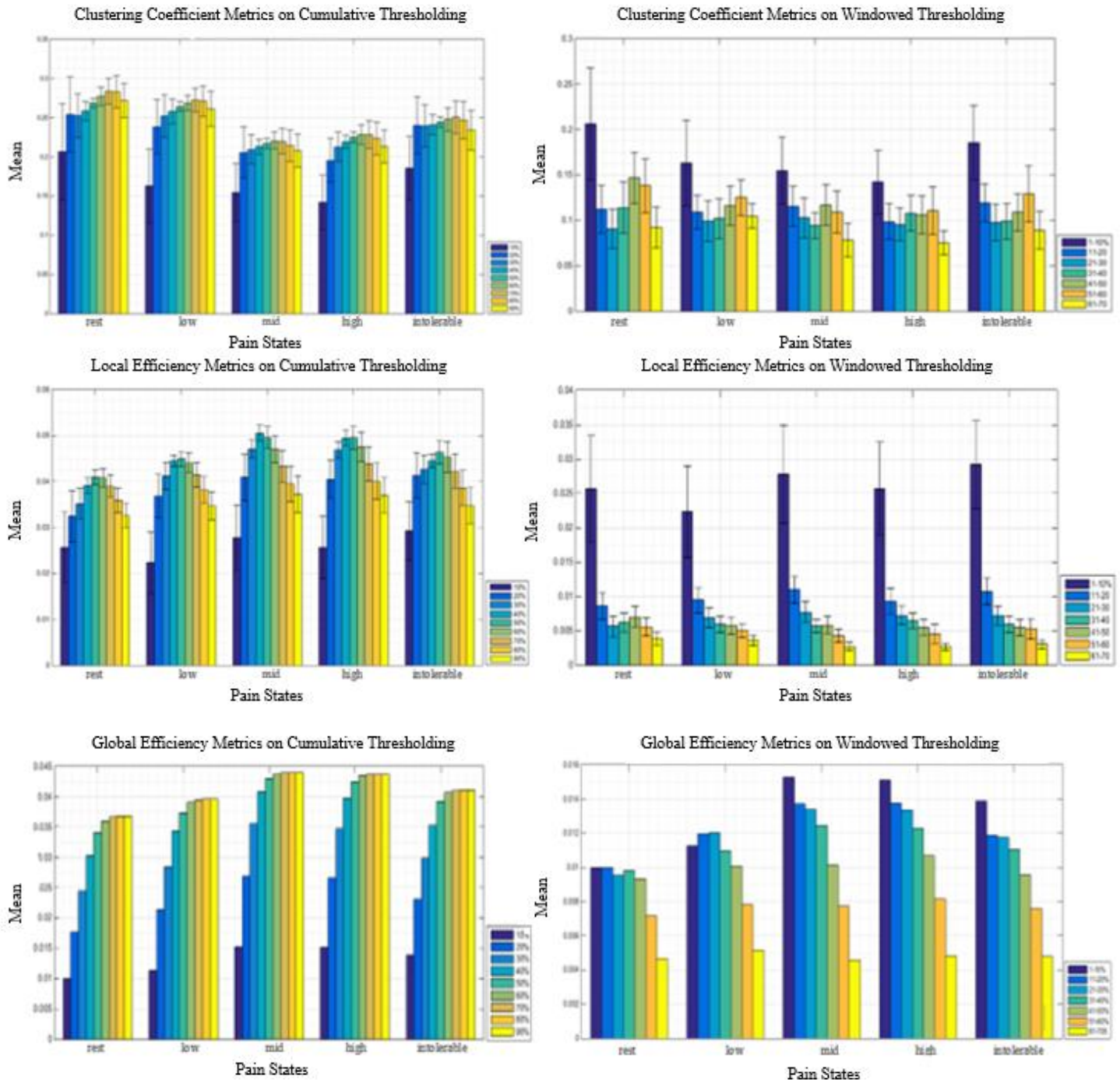
Fig. 5. Network metrics (Clustering coefficient, local efficiency &global efficiency) in five pain states. Error bars depict the standard deviation of the mean across the 23 subjects.

Table 2
The SFFS selected features for each node in the proposed decision tree by SVM

Classified states	The best features in terms of accuracy
No-pain VS. Pain	Global efficiency, local efficiency
Low, medium & high VS. intolerable	Degree, betweenness
Low & medium VS. high	Degree, betweenness
Low VS. medium	Degree, betweenness

Table 3
The pain classification results by the proposed decision tree

Classified states	Accuracy ± std (%)	Specificity (%)	Sensitivity (%)
No-pain VS. Pain	92.14±0.04	90	94.29
Low, medium & high VS. intolerable	85.21±0.13	79	90.27

| Low & medium VS. high | 80±0.1 | 73.86 | 85.57 |
| Low VS. medium | 90.03±0.6 | 88 | 93.8 |

5. Robustness

Since EEG recordings in clinics are often contaminated by noise, to show the robustness of the proposed method against additive noises, we have added white noise with different intensities to the raw EEG signals and then evaluated the results in the noisy conditions.

Here, white noise with signal to noise ratios (SNRs) of 10, 20, 30 and 40dB are added to the EEGs. Results imply that by diminishing the SNR value, the results is slightly decreased as shown in Fig. 6. This little deviation of results against different intensities of additive noise implies the strong robustness of the proposed scheme.

Table 4
Comparison of Pain State Classification problems

| Source	Classified states	Method	Accuracy
Schulz & Zherdin [13]	No-pain VS. Pain	Multivariate Pattern Analysis	83%
Vatankhah et al. [6]	No-pain VS. Pain	Energy ratio approximate entropy fractal dimension Lyapunov exponent	89%
Hadjileontiadis [7]	No-pain VS. Pain	Wavelet higher-order spectral (WHOS)	90.25%
Nezam et al. [22]	No-pain VS. Pain	fractal dimension Shannon entropy approximate entropy spectral entropy	90.6%
Nezam et al. [22]	3 Levels		83%
Nezam et al. [22]	5 Levels		62%
Proposed Method	No-pain VS. Pain	Metrics extracted PDC directed connectivity	92.14%
Proposed Method	3 Levels		88.67%
Proposed Method	5 Levels		86.84%
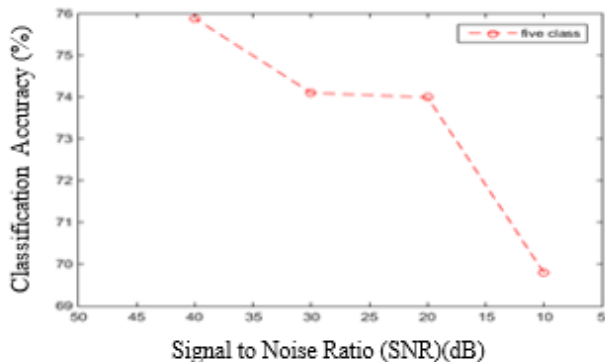
Fig. 6. Increasing the amount of Gaussian noise added to the features (which results in decreasing in SNR). Afterward, noisy test features were applied to the classifiers trained with the noisy features. As it can be seen, the selected subsets of features manifest a robust behavior versus increasing the noise level.

6. Discussion

Since feeling pain is associated with synchronization and co-activation among some parts of the brain in a certain frequency range, discovering the spatio-temporal patterns of this co-activation in different pain intensities enables us to measure the pain level. To decode the spatio-temporal patterns corresponding to different pain levels, the EEG-based functional connectivity graph of the brain is characterized by some meaningful features. Since the connections among the brain regions are dynamic and change with pain, to decode these temporal patterns, we use the directed graph features. Some of these features are used to analyze the connectivity only in a small neighborhood (e.g., with one EEG channel), while some other graph features are global and give the information about the connectivity measures among all the scalp channels. In other words, local and global connections between the brain regions are decoded for each level of pain. After extracting meaningful and tangible features, we found out that the overlap between features of different pain classes is considerably high and a single classifier cannot provide acceptable results. Consequently, a multilayer classifier in the form of a decision tree is suggested. To design the classifier structure, we carefully trace the differences between various pain levels on the brain connections illustrated in Fig. 2. Due to the strong ability of SVM for two-class tasks, a SVM is assigned to each node. This yields a significant improvement over the state-of-the-art methods.

Cognitive information processing including consolidating memory and learning predominantly takes place within the fronto-parietal network (FPN). Meanwhile, emotional processing (social communication) is largely processed in the fronto-temporal network (FTN). The primary somatosensory area is the initial cortical hub, which receives and processes the sense of pain, whereas the secondary somatosensory area (association area) participates in the process of identifying the intensity of pain. As such the process of pain perception essentially occurs within the parietal cortices.

The strong fronto-parietal brain connectivity enables instant fine motor processing, though motor reflexes not only depend on (intensity and velocity) the prefrontal cortex but also involve in tolerance and decision making. On the other hand, the insular lobe receives the pain sense as emotional and trauma as external stimuli in order to change the internal representation of external stimuli and creates different codes.

Fig. 2 reveals cognitive information processing with respect to the pain intensity level. Our findings indicate that in the moderate and high pain states, dense functional connectivity emerges within the FPN, while upon intolerable pain, the processing of emotional data evolves within FTN. While subjects are wondering for negative sensation (pain) even though upon no-pain state a robust functional connectivity continues to shape within FTN.

Given the above findings, our study strives to deploy functional brain connectivity graph features to decode the EEG information simultaneously (co-activation) and successively

(directed graph) distribute over different cortical hubs for various states of pain. Although the EEG power spectral and spatial patterns (e.g., Alpha, Beta and Delta) tend to change when pain is repeatedly investigated, to the best of authors' knowledge this is the first directed graph connectivity approach that determines the information flow patterns in pain-concurrent EEG signals. Eliciting large and small scale graph features allows us to discover the coactivity patterns of the brain subsystems in different states of pain. Taken that into account, we design a customized decision tree structure, adopting the physiological connection of the brain subsystems upon perceiving various intensities of painful stimuli. Finally, applying the features to the developed classifier provides outstanding classification accuracy on the five levels of pain. Moreover, the robustness of such features is assessed under different SNR values.

In line with what we report, a landmark study by Chen and Rappelsberger [15] highlight the fact that peripheral painful stimuli are reflected by EEG changes. The diminished EEG amplitude and simultaneous reinforced EEG coherence in the central regions are suggested to be the cortical correlates of human pain [15]. In a similar report, Chen et al [16], postulate that modular identification and delineation of the arousal–attention (located in FPN), emotion–motivation (placed in FTN) and perception–cognition (located in FPN) neural networks of pain processing in the brain are essential to our deeper understanding of how the brain processes painful stimuli. As such and similar to our investigation, brain mapping/neuroimaging studies using EEG, magnetic electroencephalography (MEG) and functional MRI (fMRI) have elaborated on the integration of sensory–motor function in pain perception [45].

In the same vein, a more recent investigation substantiate that the accuracy of EEG signal classification depended on pain-evoked responses at about 8 Hz (low alpha) oscillation with respect to the temporal–spectral pattern of pain-related neuronal responses [12]. In agreement with what they report, our results reposition EEG-informed Alpha coherence within FPN and FTN as a neuronal marker of pain sensitivity.

Such an EEG-based neuromarker would significantly be of value when patients with decreased level of consciousness or those who status-post operation in the recovery room, and well as intubated ICU-admitted patients are literally unable to express subjective pain. In line with earlier reports, the present findings may assist clinicians with objectively assessed evidence-based solutions in pain management.

The present study is subject to some limitations including a relatively small sample size and shortage of other data modalities (e.g., fMRI or MEG) which might be co-registered with our EEG data. In other words, while the analyses of oscillations are conceptually and methodologically well suited for pain investigation of the brain mechanisms of pain, evidence on the role of oscillations and synchrony in pain perception has remained scant. Future research may be needed to analyze the correspondence between EEG, MEG, and fMRI data to specify the abnormal oscillations and synchrony underlying acute and chronic pains.

The hypotheses which emerge from the present findings and deserve further testing are captivating. For instance, the question of whether similar brain-behavior dynamics are expected to be similar in patients who cannot speak with those healthy individuals who explicitly talk about their pain intensity, needs further investigations. Moreover, future works are required to examine whether the pain stimulus studied here (the cold pressure test, or CPT) is a representative stimulus of other possible pain stimuli in terms of the elicited EEG response.

7. Conclusion

In this paper, we have derived efficient features from the functional connectivity graph of EEG channels, in the Alpha band, in order to finely classify five classes of thermal pain. PDC features in two different graph scales are extracted. These features are degree, betweenness, clustering coefficient, local efficiency and global efficiency of the estimated graphs. As far as the features of pain classes have a high overlap, a single classifier is not able to perform this task. Therefore, a bio-inspired decision tree is customized for this problem and due to a large number of the generated features, a feature selection method is applied to reduce the complexity for the classification stage. The classification result for two-class state (pain versus no-pain) produces 92% accuracy while this result for the five-class state has slightly decreased to 86% accuracy. This slight decline implies the robustness of the proposed method. Moreover, results of the proposed method for different number of pain classes statistically outperform state-of-the-art schemes for the same number of classes.

Declaration of Conflicts of Interest

The authors have no conflict of interest to disclose.

References

[1] Ong, W. Y., Stohler, C. S., & Herr, D. R., Role of the prefrontal cortex in pain processing. Molecular neurobiology, 56(2), pp. 1137-1166, 2019

[2] Garra, G., Singer, A. J., Taira, B. R., Chohan, J., Cardoz, H., Chisena, E., & Thode Jr, H. C., Validation of the Wong-Baker FACES pain rating scale in pediatric emergency department patients, Academic Emergency Medicine, 17(1), pp. 50–54, 2010

[3] Hjermstad, M. J., Fayers, P. M., Haugen, D. F., Caraceni, A., Hanks, G. W., Loge, J. H., & European Palliative Care Research Collaborative (EPCRC)., Studies comparing Numerical Rating Scales, Verbal Rating Scales, and Visual Analogue Scales for assessment of pain intensity in adults: a systematic literature review, Journal of Pain and Symptom Management, 41(6), pp. 1073–1093, 2011

[4] Panavaranan, P., & Wongsawat, Y., EEG-based pain estimation via fuzzy logic polynominal kernel support vector machine, 6th Biomedical Engineering International Conference, pp. 1-4, 2013

[5] Vatankhah, M., Asadpour, V., & Fazel-Rezai, R., Perceptual pain classification using ANFIS adapted RBF kernel support vector machine for therapeutic usage, Applied Soft Computing, 13(5), pp. 2537–2546, 2013

[6] Vatankhah, M., & Toliyat, A., Pain level measurement using discrete wavelet transform, International Journal of Engineering and Technology, 8(5), pp. 380, 2016

[7] Hadjileontiadis, L. J., EEG-based tonic cold pain characterization using wavelet higher-order spectral features, IEEE Transactions on Biomedical Engineering, 62(8), pp. 1981-1991, 2015

[8] Kutluk, A., Hirano, H., Nakamura, R., Saeki, N., Yoshizumi, M., Kawamoto, M., & Tsuji, T., Assessment of pain with mechanical nociceptive stimuli by the change of arterial wall impedance, 5th International Conference on Biomedical Engineering and Informatics, pp. 451-454, 2012

[9] Afrasiabi, S., Boostani, R., & Masnadi-Shirazi, M. A., Differentiation of pain levels by deploying various electroencephalogram synchronization features and a dynamic ensemble selection mechanism, Physiological Measurement 41 (11), p. 115004, 2020

[10] Afrasiabi, S., Boostani, R., & Masnadi-Shirazi, M. A., A physiological-inspired classification strategy to classify five levels of pain, 26th National and 4th International Iranian Conference on Biomedical Engineering (ICBME), pp. 106-111, 2019

[11] Cleeland, C. S., Nakamura, Y., Howland, E. W., Morgan, N. R., Edwards, K. R., & Backonja, M., Effects of oral morphine on cold pressor tolerance time and neuropsychological performance, Neuropsycho-pharmacology, 15(3), pp. 252-262, 1996

[12] Egsgaard, L. L., Wang, L., & Arendt-Nielsen, L., Volunteers with high versus low Alpha EEG have different pain–EEG relationship: A human experimental study, Exp Brain Res, 193(3), 2009

[13] Schulz, E., & Zherdin, A., Decoding and individual`s sensitivity to pain from the multivariate analysis of EEG data, Cereb Cortex, 22(5), pp. 1118-1123, 2012

[14] Shao, S., Shen, K., Yu, K., Wilder-Smith, E. P., & Li, X., Frequency-domain EEG source analysis for acute tonic cold pain perception, Clinical Neurophysiology, 123(10), pp. 2042-2049, 2012

[15] Chen, A. C., & Rappelsberger, P., Brain and human pain: topographic EEG amplitude and coherence mapping, Brain Topography, 7(2), pp. 129-140, 1994

[16] Chen, A. C., Rappelsberger, P., & Filz, O., Topology of EEG coherence changes may reflect differential neural network activation in cold and pain perception, Brain Topography, 11(2), pp. 125-132, 1998

[17] Ferracuti, S., Seri, S., Mattia, D., & Cruccu, G., Quantitative EEG modifications during the cold water pressor test: hemispheric and hand differences, International Journal of Psychophysiology, 17(3), pp. 261-268, 1994

[18] Chen, A. C., Dworkin, S. F., Haug, J., & Gehrig, J., Topographic brain measures of human pain and pain responsivity, Pain, 37(2), pp. 129-141, 1989

[19] Fattahi, D., Nasihatkon, B., & Boostani, R., A general framework to estimate spatial and spatio-spectral filters for EEG signal classification, Neurocomputing, 119, pp. 165-174, 2013

[20] Gram, M., Graversen, C., Olesen, S. S., & Drewes, A. M., Dynamic spectral indices of the electroencephalogram provide new insights into tonic pain, Clinical Neurophysiology, 126(4), pp. 763-771, 2015

[21] Peng, W., Babiloni, C., Mao, Y., & Hu, Y., Subjective pain perception mediated by alpha rhythms, Biological Psychology, 109, pp. 141-150, 2015

[22] Nezam, T., Boostani, R., Abootalebi, V., & Rastegar, K., A novel classification strategy to distinguish five levels of pain using the EEG signal features, IEEE Transactions on Affective Computing, pp. 1-9, 2018

[23] Van Den Heuvel, M.P., & Pol, H.E.H., Exploring the brain network: a review on resting-state fMRI functional connectivity, European Neuropsycho-Pharmacology, 20(8), pp. 519-534, 2010

[24] Necka, E. A., Lee, I. S., Kucyi, A., Cheng, J. C., Yu, Q., & Atlas, L. Y., Applications of dynamic functional connectivity to pain and its modulation, Pain Reports, 4(4), 2019

[25] Case, M., Zhang, H., Mundahl, J., Datta, Y., Nelson, S., Gupta, K., & He, B, Characterization of functional brain activity and connectivity using EEG and fMRI in patients with sickle cell disease, Neuroimage: Clinical, 14, pp. 1-17, 2017

[26] Bowyer, S. M., Coherence a measure of the brain networks: past and present, Neuropsychiatric Electrophysiology, 2(1), 2016

[27] Rubinov, M., & Sporns, O., Complex network measures of brain connectivity: uses and interpretations, Neuroimage, 52(3), pp. 1059-1069, 2010

[28] Boostani, R., & Sabeti, M., Optimising brain map for the diagnosis of schizophrenia, International Journal of Biomedical Engineering and Technology, 28(2), pp. 105-119, 2018

[29] Karimzadeh, F., Boostani, R., Seraj, E., & Sameni, R., A distributed classification procedure for automatic sleep stage scoring based on instantaneous electroencephalogram phase and envelope features, IEEE Transactions on Neural Systems and Rehabilitation Engineering, 26(2), pp. 362-370, 2018

[30] Gómez-Herrero, G., Automatic artifact removal (AAR) toolbox v1. 3 (Release 09.12.2007) for MATLAB, Tampere University of Technology, 2007

[31] Delorme, A., & Makeig, S., EEGLAB: An open source toolbox for analysis of single-trial EEG dynamics including independent component analysis, Journal of Neuroscience Methods, 134(1), pp. 9–21, 2004

[32] Baccalá, L. A., & Sameshima, K., Partial directed coherence: a new concept in neural structure determination, Biological Cybernetics, 84(6), pp. 463–474, 2001

[33] Wehling, S., Simion, C., Shimojo, S., & Bhattacharya, J., Assessment of connectivity patterns from multivariate time series by partial directed coherence, Chaos Complexity Letters, 2(2-3), pp. 413–433, 2007

[34] Sakkalis, V., Review of advanced techniques for the estimation of brain connectivity measured with EEG/MEG, Computers in Biology and Medicine, 41(12), pp. 1110-1117, 2011

[35] Schneider, T., & Neumaier, A., Algorithm 808: ARfit—A Matlab package for the estimation of parameters and eigenmodes of multivariate autoregressive models, ACM Transactions on Mathematical Software (TOMS), 27(1), pp. 58-65, 2001

[36] Schwarz, G., Estimating the dimension of a model, The Annals of Statistics, 6(2), pp. 461–464, 1978

[37] http://econnectome.umn.edu/

[38] Achard, S., Bassett, D. S., Meyer-Lindenberg, A., & Bullmore, E., Fractal connectivity of long-memory networks, Physical Review E, 77(3), 2008

[39] Bullmore, E. T., & Bassett, D. S., Brain graphs: graphical models of the human brain connectome, Annual Review of Clinical Psychology, 7, pp. 113-140, 2011

[40] Schwarz, A. J., & McGonigle, J., Negative edges and soft thresholding in complex network analysis of resting state functional connectivity data, NeuroImage, 55 (3), pp. 1132–1146, 2011

[41] Boccaletti, S., Latora, V., Moreno, Y., Chavez, M., & Hwang, D. U., Complex networks: Structure and dynamics, Physics Reports, 424(4-5), pp. 175-308, 2006

[42] Stam, C. J., & Reijneveld, J. C., Graph theoretical analysis of complex networks in the brain, Nonlinear Biomedical Physics, 1(3), pp. 1753-4631, 2007

[43] Bassett, D.S., & Bullmore, E.T., Human brain networks in health and disease, Current Opinion in Neurology, 22, pp. 340–347, 2009

[44] Pudil, P., Novovičová, J., & Kittler, J., Floating search methods in feature selection, Pattern Recognition Letters, 15(11), pp. 1119–1125, 1994

[45] Chen, A. C., New perspectives in EEG/MEG brain mapping and PET/fMRI neuroimaging of human pain, International Journal of Psychophysiology, 42(2), pp. 147-59, 2001

[46] Afrasiabi, S., Boostani, R., Masnadi-Shirazi, M. A., & Nezam, T., An EEG Based Hierarchical Classification Strategy to Differentiate Five Intensities of Pain, Expert Systems with Applications, 180, p.115010180, 2021